06

Formation of SiO_2/Al_2O_3 thread-like nanostructures on the surface of Al particles and their influence on the thermomechanical properties of the Al composite

© U.U. Narzulloev, A.T. Matveev, D.V. Shtansky

National University of Science and Technology MISiS, Moscow, Russia
E-mail: matveev.at@misis.ru

Received December 16, 2025
Revised January 20, 2026
Accepted January 21, 2026

Al-matrix composites reinforced with SiO_2/Al_2O_3 thread-like nanostructures were synthesized. The composites exhibit high strength and ductility at temperatures of 25 and 500 °C. The problem of uniformly distributing the strengthening ceramic phase throughout the composite was solved by growing oxide nanostructures on the surface of metal powder particles. SiO_2/Al_2O_3 thread-like nanostructures approximately 1 μm long and less than 100 nm thick were formed at 900 °C on the surface of pre-oxidized micro-sized Al powder coated with Na_2SiO_3 from an aqueous solution.

Keywords: thread-like nanostructures, aluminum oxide, microstructure, dispersion strengthening, tensile and compressive strength.

DOI: 10.61011/TPL.2026.05.63290.20602

Due to their high strength-to-weight ratio, aluminum alloys are widely used in automotive and aviation industries. However, a sharp decrease in strength of these alloys with an increase in temperature limits their application significantly [1]. Addition of a disperse ceramic phase is one of the key methods for increasing high-temperature strength of aluminum and aluminum alloys [2]. However, dispersion strengthening of metals, specifically when using ceramic nanoparticles, faces the challenge of uniform nanoparticle distribution in the matrix. Nanoparticles are prone to agglomeration, leading to reduction of composite material strength. For uniform distribution of ceramic nanostructures in a metal matrix, a new approach has been proposed where ceramic nanoparticles were formed on the surface of metal particles. This concept has been illustrated by formation of filamentary crystals through interaction between the oxidized surface of Al particles and $LiNO_3$ [3]. The proposed approach avoids the homogenizing grinding stage, which is of practical importance. However, the strength of resulting composites has grown insignificantly due to a low mass fraction of nanostructures in the matrix (less than 1 mass%). Mass fraction of nanostructures in a composite material can be increased by using finer metal particles and by increasing the density of nanostructures on the surface of metal particles.

This study used aluminum particles smaller than 10 μm, and Na_2SiO_3 was used as reaction oxide. Interaction between Na_2SiO_3 and Al_2O_3 can form various phases in the Al_2O_3/SiO_2 and Al_2O_3/Na_2O systems, facilitating an increase in the surface density of nanostructures.

Al (1–10 μm) particle powder was pre-oxidized at 600 °C during 180 min, then wetted in water-alcohol solution of Na_2SiO_3 and annealed at a high temperature of 900 °C during 60 min. According to the scanning electron microscopy (SEM) data (JSM-7600F, JEOL, Japan), filamentary nanostructures about 1 μm in length and less than 100 nm in thickness were formed on the surface of Al particles (Figure 1, *a*). According to the energy-dispersive X-ray spectroscopy data, the powder contained Al, O and Si at the ratio (at.%): Al:O:Si = 45.6:53.1:1.3.

X-ray patterns of Al powder, oxidized Al powder (Al_{ox}) and Al powder with filamentary nanostructures ($Al-SiO_2$) measured on the SmartLab diffractometer (Rigaku, Japan) are shown in Figure 1, *b*. The base peaks in the diffraction patterns of Al samples (curve *1*) and Al_{ox} (curve *2*) refer to Al (ICDD 03-065-2869). The X-ray pattern of an Al_{ox} sample after Al powder oxidation contains a low-intensity broad maximum within $2\theta = 25-35°$ and weak peaks at $2\theta = 45.1$ and 66.5°, which can be referred to the γ-Al_2O_3 phase (ICDD 01-074-4629). In the $Al-SiO_2$ sample (curve *3*), additional SiO_2 peaks (ICDD 00-002-0286) occur, and intensity of peaks from the γ-Al_2O_3 phase increases. Figure 1, *c* shows SEM images of $Al-SiO_2$ containing filamentary nanostructures about 10 nm in diameter (shown by arrows) and also a nanostructure agglomerate, from which element distribution maps and a linear element distribution profile (scanning line is shown in the SEM image) could be obtained. The agglomerate shows relative decrease in the intensity of Al signal and a signal from Si and O occurs. The oxygen peak is wider than the silicon peak. This indicates that oxygen is bonded not only with Si, but also with Al. Thus, the X-ray phase and elemental analysis data show that the nanostructures were formed by the SiO_2 and Al_2O_3 phases.

Annealing of Al particles at a temperature below T_{melt} ($\sim$ 630 °C) causes formation of a firm oxide shell that

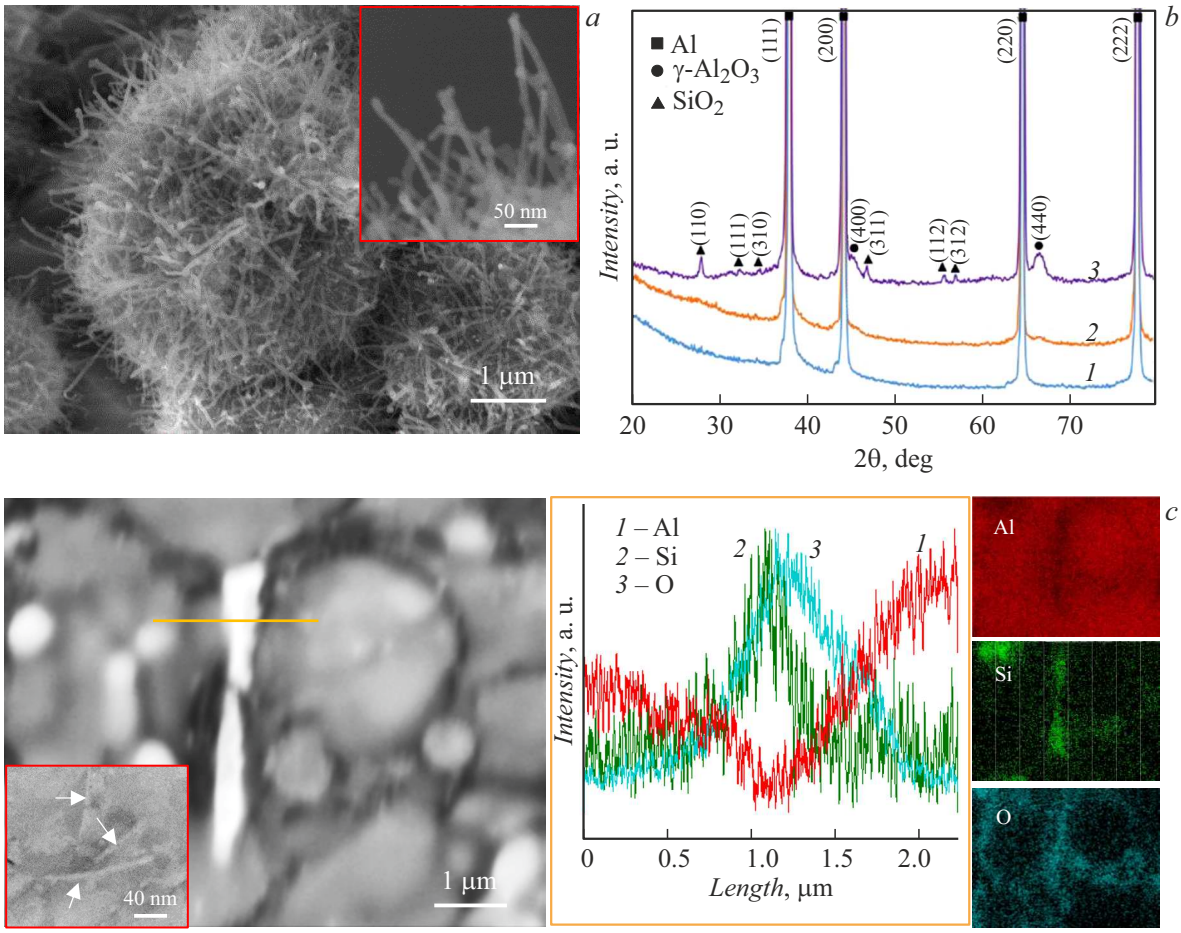

Figure 1. *a* — SEM image of Al particles with filamentary nanostructures after annealing at 900 °C during 60 min. *b* — X-ray patterns of Al powder (*1*), oxidized Al powder (*2*) and Al powder with filamentary nanostructures (*3*). *c* — SEM image of the Al–SiO_2 composite surface with filamentary nanostructures (in the inset), maps of element distribution in this region and element distribution profile in the agglomerate (scanning line is marked in the SEM image).

confines the Al melt during annealing above T_{melt}. According to the theoretical simulation data, Al_2O suboxides are formed at the Al_2O_3/Al_{melt} internal interface, which, under the excess pressure in particles, diffuse through oxide shell nanopores to the surface where they disproportionate to Al and Al_2O_3 and form $Al@Al_2O_3$ nanowires [4]. Usage of sodium silicate on the surface of oxidized aluminum particles causes formation of SiO_2-based filamentary nanostructures.

Composite materials were produced from all three types of powders via the spark plasma sintering technique in vacuum using the Labox 650 SPS system (Sinter Land Inc., Japan) at 630 °C, compression pressure 49.5 MPa and sintering time 10 min. Densities and hardnesses of the samples are listed in the table. Hardness of the material with filamentary SiO_2 nanostructures is twice as high as that of the Al and Al_{ox} samples.

Figure 2 shows the UTS values and stress–strain curves for samples tested at 25 and 500 °C. Al and Al_{ox} samples have UTS, respectively, equal to 94 MPa and 101 MPa (25 °C) and to 54 MPa and 62 MPa (500 °C). This shows that oxidation of Al particles doesn't make any significant contribution to the increase in material strength and doesn't reduce material ductility. UTS of Al–SiO_2 was 212 MPa (25 °C) and 140 MPa (500 °C), which corresponds to an increase in strength by 126 % (25 °C) and 159 % (500 °C) compared with Al strength. It should be pointed out that Al–SiO_2 retained its high tensile ductility with high strength (relative elongation of about 30 % at 25 °C and 40 % at 500 °C). SEM microphotographs of fracture regions in samples after tensile testing at 25 and 500 °C recorded using the JSM-7600F (JEOL, Japan) are shown in Figure 2, *c*. All samples display a typical cellular microstructure, indicating

Density and hardness of samples prepared via spark plasma sintering from Al, oxidized Al and Al–SiO_2 powders

Sample	Density, g/cm^3	Hardness, HV_5
Al	2.68 ± 0.06	28 ± 3
Al_{ox}	2.68 ± 0.05	32 ± 2
Al–SiO_2	2.72 ± 0.06	65 ± 2

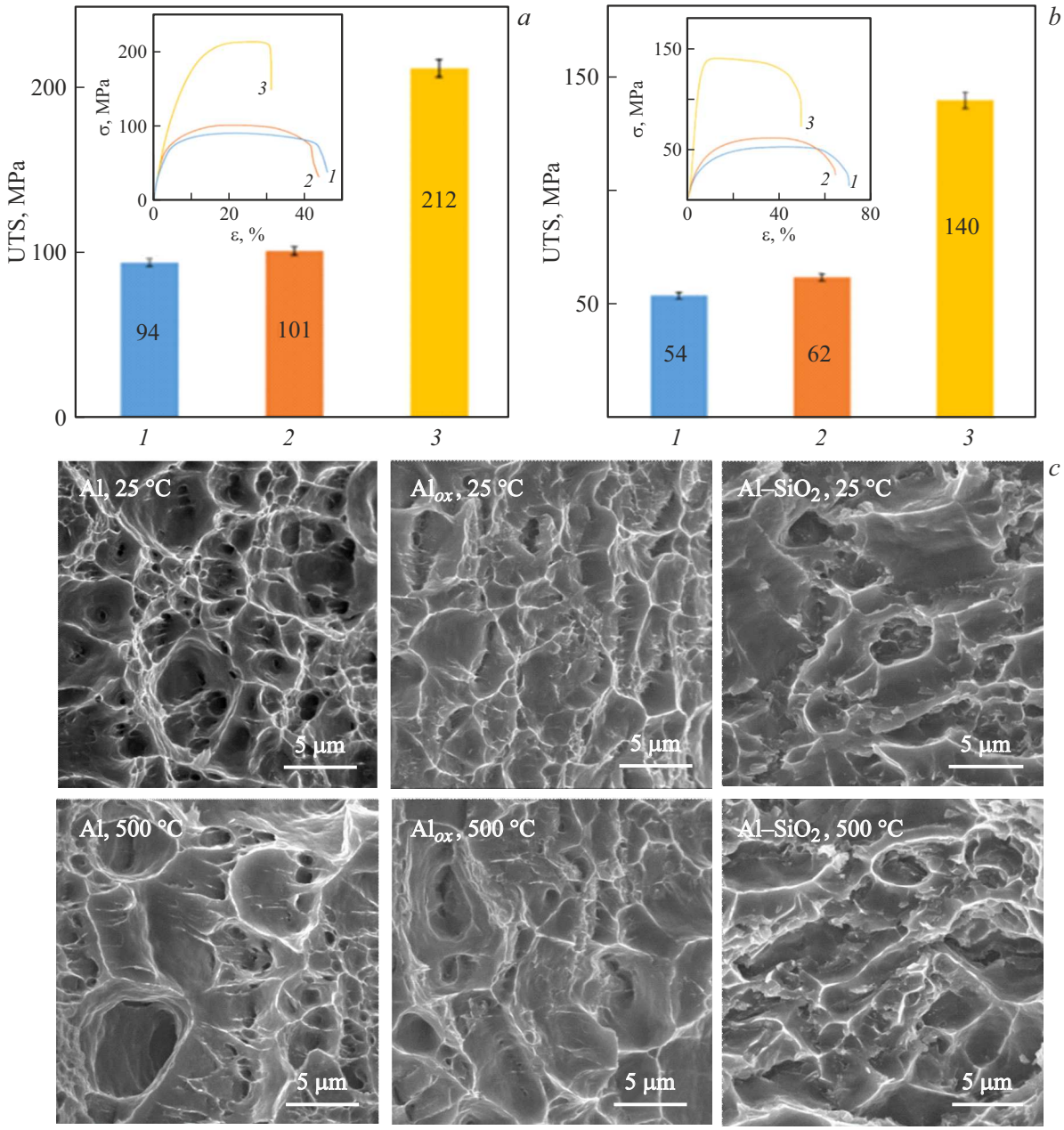

Figure 2. Ultimate tensile strength (UTS) at 25 (*a*) and 500 °C (*b*). Insets show corresponding stress–strain curves ($\sigma-\varepsilon$): *1* — Al, *2* — oxidized Al, *3* — Al–SiO_2 composite. *c* — fracture patterns of samples after tensile testing at 25 and 500 °C.

a predominantly plastic mode of fracture. This agrees well with the corresponding stress–strain curves ($\sigma-\varepsilon$).

UCS values and stress–strain curves measured at 25 and 500 °C are shown in Figure 3. Compared with UCS for the Al samples (118 MPa) and Al$_{ox}$ samples (131 MPa), UCS of the composite material with filamentary SiO_2 nanostructures at 25 °C increases to 335 MPa, which corresponds to an increase in strength by 184 % compared with the strength of Al. At 500 °C, UCS is 243 MPa, which is higher by 292 % than that of Al. As the strength of composite materials increases, their ductility generally decreases independently of the morphology of disperse strengthening phase [5,6]. Therefore it should be pointed out that Al–SiO_2 also retain their high ductility in compression: relative elongation is 28 % at 25 °C and 35 % at 500 °C.

This proves the practical relevance of the earlier proposed concept of creating dispersion-strengthened metal-matrix composite materials via oxide nanostructure growth on the surface of oxidized metal powder particles. Formation of numerous filamentary SiO_2/Al_2O_3 nanostructures about 1 μm in length and less than 100 nm in thickness on the surface of each micron-scale Al particle provides uniform distribution of nanostructures in the bulk of the composite material. Al–SiO_2 has a hardness of 65 HV_5, ultimate

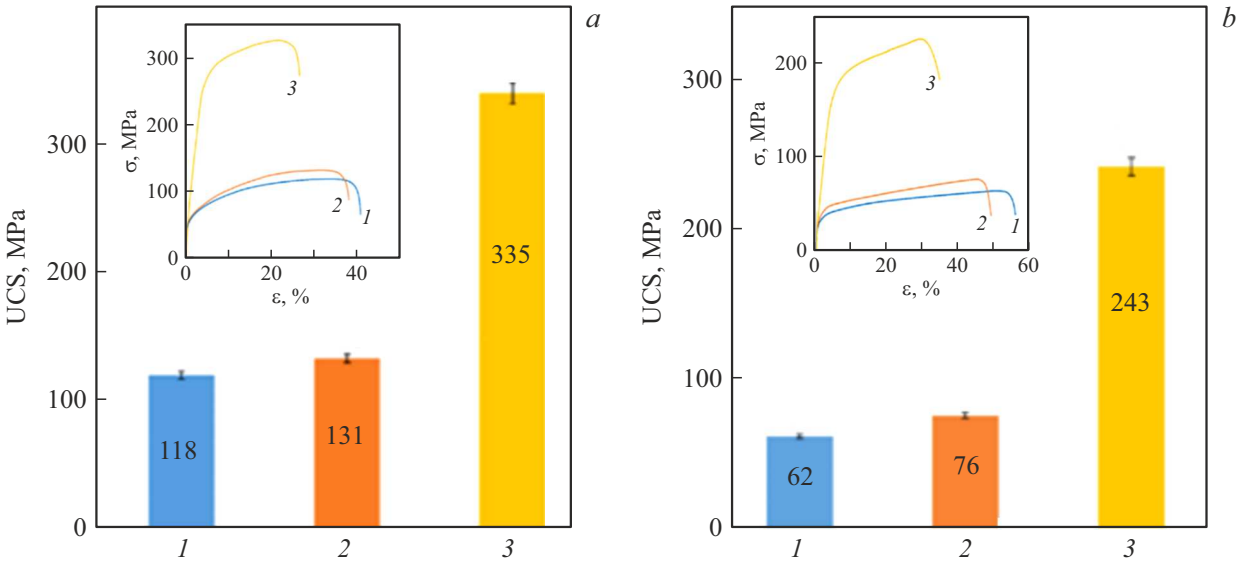

Figure 3. Ultimate compression strength (UCS) at 25 (*a*) and 500 °C (*b*). Insets show corresponding stress–strain curves ($\sigma-\varepsilon$): *1* — Al, *2* — oxidized Al, *3* — Al–SiO_2 composite.

tensile strength and ultimate compression strength of 212 MPa and 335 MPa (25 °C) and of 140 MPa and 243 MPa (500 °C) at a relative elongation greater than 28 %.

Funding

The study was funded by the Ministry of Higher Education and Science of the Russian Federation (project No FSME-2023-0004).

Conflict of interest

The authors declare no conflict of interest.

References

[1] S.-S. Li, X. Yue, Q.-Y. Li, H.-L. Peng, B.-X. Dong, T.-S. Liu, H.-Y. Yang, J. Fan, S.-L. Shu, F. Qiu, Q.-C. Jiang, J. Mater. Res. Technol., **27**, 944 (2023). DOI: 10.1016/j.jmrt.2023.09.274
[2] K. Pooja, N. Tarannum, P. Chaudhary, Discov. Mater., **5**, 35 (2025). DOI: 10.1007/s43939-025-00226-6
[3] U.U. Narzulloev, M.K. Kutzhanov, I.V. Shchetinin, P.A. Loginov, D.V. Shtansky, A.T. Matveev, Tech. Phys. Lett., **50** (5), 33 (2024). DOI: 10.61011/TPL.2024.05.58418.19847
[4] U.U. Narzulloev, A.T. Matveev, M.K. Kutzhanov, A.S. Konopatsky, I.V. Shchetinin, P.A. Loginov, L.A. Varlamova, J.J. Pais Pereda, P.B. Sorokin, D.V. Shtansky, Appl. Surf. Sci., **664**, 160223 (2024). DOI: 10.1016/j.apsusc.2024.16022
[5] R. Wang, W. Guo, L. Liu, K. Yuan, J. Wang, S. Zhao, L. Chen, J. Mater. Res. Technol., **23**, 191 (2023). DOI: 10.1016/j.jmrt.2022.12.187
[6] H. Zhu, Z. Liu, X. Li, H. Liu, X. Wang, J. Hou, Z. Liu, B. Xiao, Z. Ma, Z. Zhang, Composites A, **200**, 109320 (2026). DOI: 10.1016/j.compositesa.2025.109320

Translated by E.Ilyinskaya